

TECHNICAL NOTE

Lee Hulse-Smith,¹ M.S. and Mike Illes²

A Blind Trial Evaluation of a Crime Scene Methodology for Deducing Impact Velocity and Droplet Size from Circular Bloodstains*

ABSTRACT: In a previous study, mechanical engineering models were utilized to deduce impact velocity and droplet volume of circular bloodstains by measuring stain diameter and counting spines radiating from their outer edge. A blind trial study was subsequently undertaken to evaluate the accuracy of this technique, using an applied, crime scene methodology. Calculations from bloodstains produced on paper, drywall, and wood were used to derive surface-specific equations to predict 39 unknown mock crime scene bloodstains created over a range of impact velocities (2.2–5.7 m/sec) and droplet volumes (12–45 μL). Strong correlations were found between expected and observed results, with correlation coefficients ranging between 0.83 and 0.99. The 95% confidence limit associated with predictions of impact velocity and droplet volume was calculated for paper (0.28 m/sec, 1.7 μL), drywall (0.37 m/sec, 1.7 μL), and wood (0.65 m/sec, 5.2 μL).

KEYWORDS: forensic science, bloodstain pattern analysis, blood drop, spines

It is not unusual to find bloodstain patterns in association with a violent encounter and through proper interpretation they can provide critical details regarding such an event. Criminalists, however, are limited by a number of variables that are unavailable for crime scene reconstruction. These variables include blood droplet volume and surface impact velocity. Accurate calculations for each could estimate the release height of passive droplets, the characteristics of the release surface, and the forces involved in bloodshed.

Previous attempts to deduce impact velocity using bloodstain diameter have been unsuccessful because bloodstain diameter is primarily dependent on two unknown variables (droplet size and velocity). Given these results, investigators are cautioned from using bloodstain measurements to infer impact velocity. As a result, two classification systems have emerged that broadly group bloodstains into either velocity (low, medium, high) or diameter (fine, small, medium, large) categories (1,2).

A second independent variable is required to determine these unknown droplet properties. Spines, commonly found to be radiating from the periphery of circular bloodstains (Fig. 1) and created at the moment of impact due to pressure instabilities (3), represent this second variable. Balthazard et al. (4) first conducted a detailed study of bloodstain spines in 1939. This research found that the number of spines directly correlated to release height and droplet volume. They could not, however, separate the effects of

each property and therefore concluded that a deeper understanding of droplet impact was required.

Since then, fluid mechanics have provided a clearer picture of droplet impact dynamics. Many analytical models have been developed that clearly show a predictable relationship between droplet properties (velocity and size) and stain morphology (diameter and spine quantity) (3,5–8). These models typically utilize two dimensionless variables, the Weber and Reynolds numbers, which represent the various opposing forces that a droplet experiences at the moment of impact. These forces include those that promote droplet spreading (density, impact velocity, and droplet volume) and those that resist spreading (surface tension and viscosity).

In a previous study, we utilized high-speed photography to examine blood droplet impact, 90° to three target surfaces (9). Strong similarities were discovered between blood and other fluids with respect to droplet spreading and spine formation. Based on these observations, experimental results were fitted to mathematical models in order to derive two equations that could solve for droplet properties. These equations proved highly supportive for the use of bloodstain diameter and spine quantity in predicting droplet volume and impact velocity. However, a constant was utilized to offset variability caused by surface irregularities, spine quantification, and blood physical properties. These factors would have to be addressed before implementation within a criminal investigation.

The purpose of the study described here was to evaluate the utility of this methodology using a modified protocol that is both amendable to crime scene analysis and can address previously observed variability. This protocol was then subjected to a blind trial evaluation under mock crime scene conditions.

Material and Methods

Venous blood was drawn from two volunteers by a qualified medical technologist into glass tubes containing EDTA and stored

¹Centre of Forensic Sciences, 25 Grosvenor Street, Toronto, ON, Canada M7A 2G8.

²Ontario Provincial Police, 453 Landsdowne Street East, Peterborough, ON, Canada K9J 6X5.

*Presented at the 2005 Annual Meeting of the American Academy of Forensic Sciences, February, Seattle, WA, U.S.A.

Received 3 Dec. 2005; and in revised form 17 June 2006; accepted 1 July 2006; published 8 Dec. 2006.

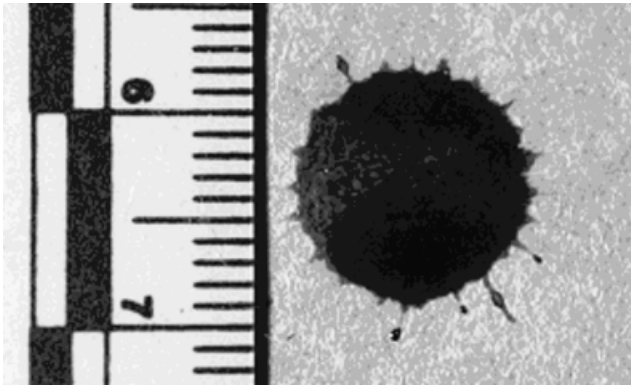


FIG. 1—Spines are shown radiating from the outer rim of a circular bloodstain on a paper surface. Droplet volume and impact velocity were 12.8 μL and 4.83 m/sec, respectively. Scale bar increments are in millimeters.

at -4°C for no more than 5 days before experimentation. One blood sample was designated for the mock crime scene and the other was used for blood calibrations.

Mock Crime Scene

The mock crime scene was created as follows: stock blood was brought to room temperature and drawn into a glass syringe fitted with one of three stainless-steel, flat-bottomed, hypodermic needles to create variations in droplet volume. The syringe was mounted to an adjustable laboratory stand to allow for variations in release height. Release height was measured between the test surface and the needle tip. Fifty-one blood droplets were made to impact at 90° to three different surfaces (paper, drywall, and wood). The selection of both release height (10–177 cm) and droplet volume (12, 25, 45 μL) was purely random. Blood droplets were released very slowly by manually depressing the plunger so that droplets were released from the needle under their own weight. The needle was cleaned periodically with a tissue to prevent blood from drying at the tip. The syringe was also frequently inverted to prevent settling of red blood cells. The resulting stains were allowed to dry before photography, using a standard digital color camera. Along with the bloodstain, each image included a scale bar and a randomly assigned bloodstain identification number.

Bloodstain Calibration

A second individual with no prior knowledge of the mock crime scene conditions was selected to gather the bloodstain calibration data required for droplet predictions. This individual was provided with only the 51 crime scene photographs and samples of the three crime scene surfaces.

Bloodstain calibration data were gathered as follows: the second human blood source was removed from storage at -4°C and brought to room temperature. A glass syringe, fitted with a stainless-steel, flat-bottomed, hypodermic needle (inner diameter 1.1 mm, outer diameter 1.4 mm), was used to aspirate 2–4 mL of blood. The syringe was then mounted to a laboratory stand in order to accommodate various release heights. Seven to 10 release heights were selected, ranging from 10 and 170 cm, to cover droplet release from a human body. In order to expand the calibration range, a smaller-diameter needle was selected (inner diameter 0.55 mm, outer diameter 0.8 mm) for additional release heights between 10 and 30 cm, and a larger-diameter needle was selected (inner diameter 2.2 mm, outer diameter 2.7 mm) for ad-

ditional release heights between 150 and 170 cm. Alternatively, a wider height range could have been selected. If it was later determined that a crime scene bloodstain fell outside the calibration range, the range could simply be expanded with additional calibration impacts.

Each crime scene surface was placed beneath the syringe on a flat-laboratory bench to accommodate impact at 90° . Droplets were released and bloodstains were photographed as previously described. Each impact was repeated three times. These methods were repeated for the other two crime scene surfaces.

Results and Discussion

Table 1 shows the bloodstain calibration results generated for each surface. Droplet volume was calculated by dividing a 4-mL blood volume by the number of droplets it produced for each stainless-steel needle. Droplet volume was then converted to a diameter value. Our previous work that examined volume variation between droplet release was shown by high-speed photography to be minimal (9). Impact velocity was calculated using release height and the following formula:

$$V_0 = \sqrt{2gh} \quad (1)$$

where g is acceleration due to gravity and h is the release height.

Bloodstain properties, shown in Table 1, were documented by digital photographs taken after each calibration stain had dried onto the target surface. Stain diameter was measured using public domain NIH image program (U.S. National Institute of Health, Bethesda, MD). A pixel threshold was first established to measure each bloodstain area before converting this value to a stain diameter. The bloodstain area did not include spines. Determining spine quantity was more subjective. A spine was defined as any deviation from an otherwise smooth outer circumference. This definition included shapes, such as waves, spikes, and triangles. Next, it was decided that only one person should count both the crime scene and calibration bloodstain spines, eliminating possible conflicting opinions regarding the existence of a spine. The number of spines was then counted around the entire bloodstain.

A number of important variables are shown in Table 1. These variables include the spread factor and two inertia variables. The spread factor is calculated by dividing the stain diameter by the droplet diameter and is used to normalize bloodstain size for comparative purposes. The two inertia values are central to generating calibration data. They are based on the Weber (We) and Reynolds (Re) dimensionless numbers (Eqs. [2] and [3]) but have been modified by removing the physical blood property variables, such as density (ρ), viscosity (ν), and surface tension (σ) (Eqs. [4] and [5]). The variables that remain include droplet volume (D_0) and impact velocity (V_0).

$$We = \frac{\rho D_0 V_0^2}{\sigma} \quad (2)$$

$$Re = \frac{\rho D_0 V_0}{\nu} \quad (3)$$

$$We_{(\text{mod})} = D_0 V_0^2 \quad (4)$$

$$Re_{(\text{mod})} = D_0 V_0 \quad (5)$$

Removing the blood property variables was considered acceptable as it was unlikely that they could be measured from a crime

TABLE 1—Bloodstain calibration data are shown for each surface (drywall, wood, paper).

Surface	Droplet Properties		Stain Properties			Inertia	
	Velocity (V_0) (m/s)	Diameter (D_0) ($\times 10^{-3}$ m)	Diameter (D_s) ($\times 10^{-3}$ m), $n = 3$	Spines (N), $n = 3$	Spread Factor: (D_s/D_0)	Re_{mod} ($\times 10^{-3}$)	We_{mod} ($\times 10^{-3}$)
Drywall	1.1	2.9	6.1 ± 0.4	—	2.1	3.2	3.5
	2.1	2.9	7.7 ± 0.4	17 ± 1.0	2.7	6.1	12.8
	1.0	3.5	7.1 ± 0.2	—	2.0	3.5	3.5
	2.6	3.5	10.8 ± 0.2	20 ± 2.0	3.1	9.1	23.7
	4.4	3.5	12.1 ± 0.2	23 ± 2.3	3.5	15.4	67.8
	5.3	3.5	12.6 ± 0.4	25 ± 0.6	3.6	18.6	98.3
	5.7	3.5	13.3 ± 0.6	28 ± 1.5	3.8	20.0	113.7
	5.3	4.4	17.4 ± 0.2	32 ± 1.5	4.0	23.3	123.6
	5.8	4.4	17.6 ± 0.7	31 ± 2.3	4.0	25.5	148.0
Wood	1.1	2.9	7.2 ± 0.1	—	2.5	3.2	3.5
	2.1	2.9	9.7 ± 0.5	—	3.3	6.1	12.8
	1.2	3.5	8.9 ± 0.4	—	2.5	4.2	5.0
	2.9	3.5	12.2 ± 0.5	—	3.5	10.2	29.4
	4.3	3.5	13.6 ± 0.5	—	3.9	15.1	64.7
	4.9	3.5	15.1 ± 0.6	28 ± 1.2	4.3	17.2	84.0
	5.7	3.5	14.8 ± 0.4	32 ± 2.6	4.2	20.0	113.7
	5.8	4.4	19.2 ± 0.6	37 ± 2.6	4.4	25.5	148.0
	Paper	1.0	2.9	5.6 ± 0.3	—	1.9	2.9
2.7		2.9	8.3 ± 0.2	14 ± 0.6	2.9	7.8	21.1
1.1		3.5	7.2 ± 0.3	—	2.1	3.9	4.2
3.7		3.5	12.3 ± 0.5	23 ± 2.0	3.5	13.0	47.9
4.6		3.5	12.8 ± 0.2	23 ± 1.5	3.7	16.3	74.1
5.2		3.5	13.5 ± 0.3	26 ± 2.6	3.9	18.3	94.6
5.8		3.5	13.4 ± 0.3	28 ± 1.0	3.8	20.2	117.7
5.2		4.4	17.0 ± 0.6	32 ± 2.0	3.9	23.0	119.0
5.8		4.4	17.1 ± 0.2	35 ± 1.5	3.9	25.4	148.0

Several droplets of varying properties (velocity, volume) were made to impact onto each surface. Bloodstain properties (diameter, spines) were documented from digital images of each calibration bloodstain. Replicates of three were used to calculate the mean and standard deviation. The spread factor was calculated as a ratio of the stain and droplet diameter. Two inertia values (We_{mod} , Re_{mod}) related to the droplet properties were also calculated for each bloodstain (Eqs. [4] and [5]).

scene bloodstain. To account for blood property variations, the calibration results (shown in Table 1) were gathered using a different blood source from that used to create the mock crime scene.

Nine droplet impact conditions failed to produce spines and could not therefore be used for purposes of calibration. This was especially true for the wood surface where more than half of the impact events did not result in spine formation. Without exception, these conditions were specific to a reduction in droplet inertia, consistent with previous research demonstrating that a surface-specific inertia threshold must be surpassed before spines are visible (10). The inertia threshold is dependent on surface characteristics, such as roughness and wettability. If inertia falls below the threshold, these surface characteristics will be insuffi-

cient to retain spines once the spreading droplet has reached its maximum diameter and has begun to recoil. The results shown in Fig. 2 highlight this effect. Bloodstains, generated using similar droplet volumes and release heights, are shown for each surface. The bloodstain on wood (Fig. 2A) shows a nearly smooth outer rim, while the bloodstains on paper (Fig. 2B) and drywall (Fig. 2C) resulted in the generation of clearly visible spines.

The results shown in Table 1 were used to generate two calibration graphs for each surface. Figures 3 and 4 show the calibration graphs for paper. The two graphs compare the spread factor (D_s/D_0) and spine quantity (N) for the Weber- and Reynolds-modified numbers, respectively. Presenting the data in this way revealed a positive correlation between the bloodstain

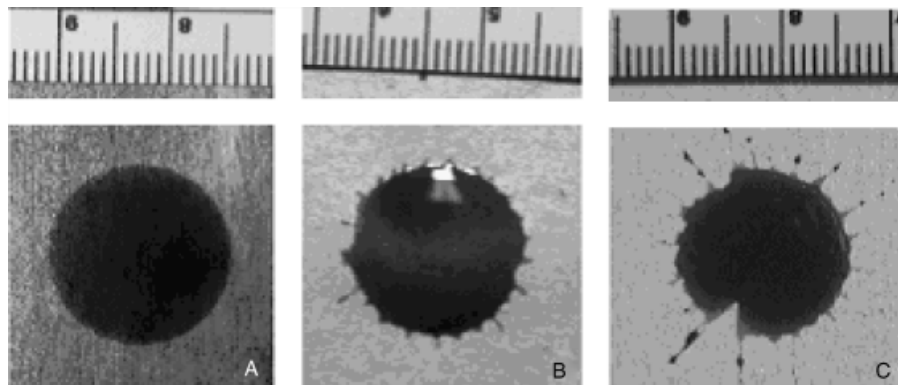


FIG. 2—Bloodstains are shown on three different surfaces to highlight their effect on spines. A similar droplet volume and impact velocity was used for (A) wood (44.6 μ L, 4.1 m/sec), (B) paper (44.6 μ L, 3.9 m/sec), and (C) drywall (44.6 μ L, 4.2 m/sec). Scale bar increments were in millimeters. Bloodstains were photographs from directly above. Image sizes have been synchronized to allow for a direct comparison.

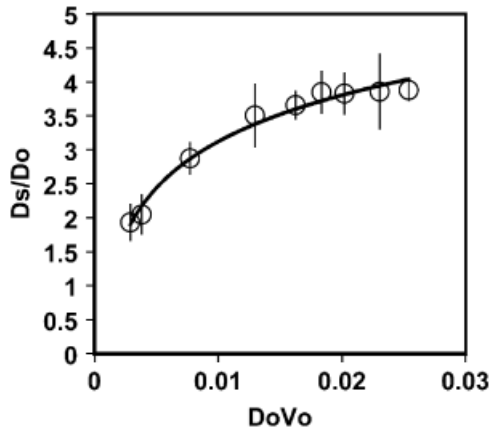


FIG. 3—Calibration data for paper (Table 1) were used to plot the diameter ratio (D_s/D_0) against the Reynolds modification number (D_0V_0). Scale bars represent the standard deviation ($n = 3$). A logarithmic trend line is fitted to the data points.

variables (stain diameter and spine quantity) and droplet inertia. A best-fit line was applied to the data points in Figs. 3 and 4, resulting in two equations that solve for bloodstain diameter and the number of spines (Eqs. [6] and [7]). The linear trend, shown in Fig. 4, was unexpected, considering that previous research predicted a logarithmic relationship. A direct comparison was difficult, however, as these calibration results were designed to be surface-specific.

$$\frac{D_s}{D_0} = 13.8\sqrt[3]{D_0V_0} \quad (6)$$

$$N = 146D_0V_0^2 + 12.8 \quad (7)$$

Droplet volume and impact velocity were then solved algebraically using Eqs. (6) and (7). These equations are shown below for paper (Eqs. [8] and [9]). The same method was also applied to derive equations for wood and drywall (not shown).

$$D_0 = 0.38\left(\frac{D_s}{\sqrt[3]{N}}\right)^{6/7} \quad (8)$$

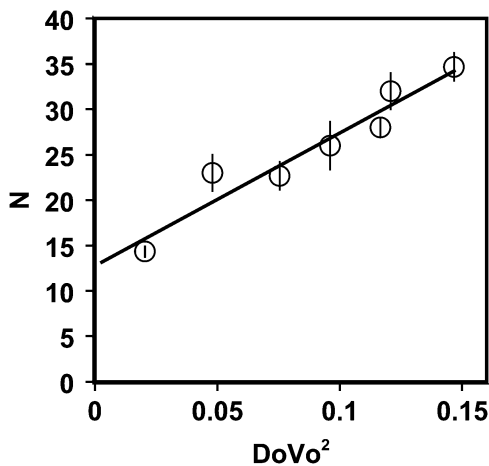


FIG. 4—Calibration data for the paper surface (Table 1) are used to plot the number of spines (N) against the Weber modification number ($D_0V_0^2$). Scale bars represent the standard deviation ($n = 3$). A linear trend line is fitted to the data points.

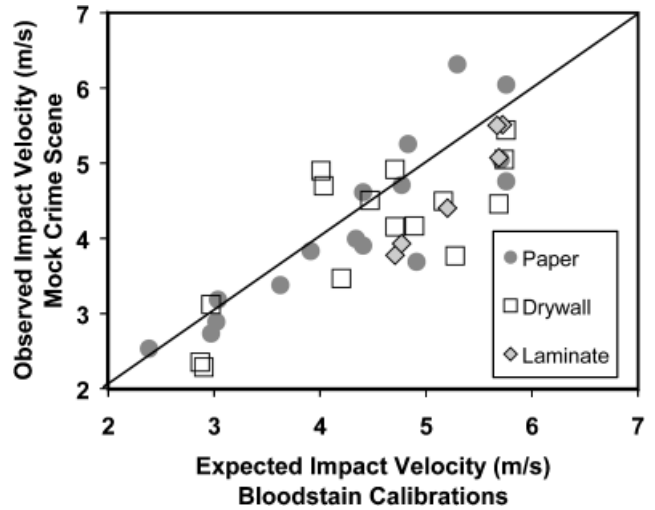


FIG. 5—Impact velocity predictions for each surface (paper, drywall, wood) are compared against actual values from the mock crime scene bloodstains.

$$V_0 = 0.019\left(\frac{N^{8/3}}{D_s}\right)^{6/14} \quad (9)$$

The two equations derived for each surface were used to predict impact velocity and droplet volume for the corresponding mock crime scene bloodstains. The bloodstain diameter and number of spines were first measured from the mock crime scene images using previously described methods. Mock crime scene bloodstains without spines (nine of 51) and bloodstains that fell outside the calibration range (based on stain diameter and spine quantity, three of 51) were excluded before making such predictions.

Expected and observed results for impact velocity and droplet volume are compared in Figs. 5 and 6 for each surface. Statistical analysis, shown in Table 2, reveals a strong linear correlation for each surface, with correlation coefficients ranging between 0.83 and 0.99. These results confirm that bloodstain measurements can be combined in order to predict both impact velocity and droplet volume. In addition, the consequences of this correlation form the

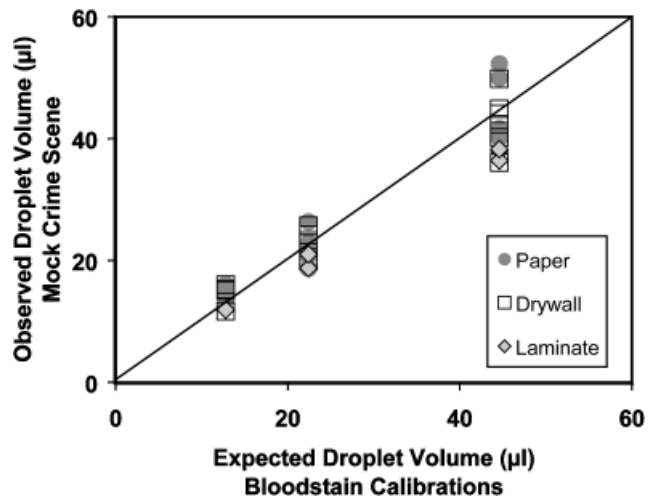


FIG. 6—Droplet volume predictions for each surface (paper, drywall, wood) are compared against actual values from the mock crime scene bloodstains. Three droplet volumes were utilized when creating the mock crime scene.

TABLE 2—Statistical analysis of mock crime scene predictions (impact velocity, droplet volume) are calculated according to surface.

	Drywall		Paper		Wood	
	Impact Velocity	Droplet Volume	Impact Velocity	Droplet Volume	Impact Velocity	Droplet Volume
Sample size	16	16	17	17	6	6
Range	2.2–5.7 m/sec	12–45 μ L	2.3–5.7 m/sec	12–45 μ L	4.7–5.7 m/sec	12–45 μ L
Correlation coefficient	0.83	0.97	0.90	0.97	0.97	0.99
95% CI	0.37 m/sec	1.7 μ L	0.28 m/sec	1.7 μ L	0.65 m/sec	5.2 μ L

basis for three general trends when comparing circular bloodstains on the same crime scene surface before performing a calibration:

- (1) Where the larger bloodstain has fewer spines, it will have derived from a larger droplet impacting at a lower velocity.
- (2) Where the larger bloodstain has greater spines, it will have derived from a larger droplet impacting at a higher velocity.
- (3) Bloodstains without spines, or on different surfaces, cannot be compared in this manner.

Further research will be required to confirm these trends, and to evaluate whether they remain valid beyond this experimental range.

The variability in droplet volume and impact velocity prediction is shown in Table 2 for each surface. With the exception of wood, variability was relatively low with a maximum 95% confidence limit of 0.37 m/sec and 1.7 μ L. However, Figs. 5 and 6 show that variability increases with inertia. If this trend continues, it may prove difficult to calibrate high-energy droplets. For wood, only six crime scene predictions were available to assess variability. In addition, these six predictions do not appear to deviate significantly from the other two surfaces, as can be seen in Figs. 5 and 6, suggesting that the variability was not directly caused by the wood and instead, highlights the need for adequate calibration points. Overall, this level of variability would allow an investigator to resolve release heights into 20-cm intervals, and help to distinguish between blood dripping from objects such as a knife and fingertip.

Although further research is required to confirm these trends and expand the experimental range, one advantage to using surface-specific equation is that it provides an internal quality control check. Instead of relying on external data to form a conclusion, the investigator conducts a calibration experiment specific to the surface of interest, and can verify these trends before applying them to casework stains. Overall, bloodstain pattern analysis is a complex undertaking, typically used by individuals with years of hands-on experience. It is therefore likely that future research will not only uncover novel techniques, but will provide a greater scientific foundation for many of the observations that have been accumulated through years of casework practice.

Conclusion

Both bloodstain diameter and spine quantity were utilized to derive surface-specific equations for predicting both impact velocity and droplet volume. These equations were then used to assess mock crime scene bloodstains as part of a blind trial evaluation. Strong correlations were found between expected and ob-

served results, leading to the formation of three general trends for comparing circular bloodstains on identical surfaces. Variability was found to be sufficiently low for the differentiation of both impact velocity and droplet volume within values of 0.37 m/sec and 1.7 μ L. Additional research is required to confirm these trends and expand the calibration range. Finally, it is important to note that any technique used in judicial proceedings should undergo a rigorous validation process before casework implementation.

Acknowledgments

We would like to thank Dr. Sanjeev Chandra from the University of Toronto for his constant advice and support. We are also indebted to Lynn Grant for her technical assistance with regard to acquiring and handling blood. Finally, we would like to thank the Ontario Provincial Police in Peterborough for graciously donating space and equipment.

References

1. Laber TL. Bloodspatter classification. *IABPA News* 1985;2(4):1–12.
2. MacDonell HL, Bialousz LF. Flight characteristics and stain patterns of human blood. Washington, DC: National Institute of Law Enforcement and Criminal Justice, Law Enforcement Assistance Administration, 1971.
3. Allen RF. The role of surface tension in splashing. *J Colloid Interface Sci* 1975;51(2):350–1.
4. Balthazard V, Piedelievre R, Desoille H, DeRobert L. Study of projected drops of blood. *Ann Med Leg Criminol Police Sci Toxicol* 1939;19:265–323.
5. Rein M. Phenomena of liquid drop impact on solid and liquid surfaces. *Fluid Dyn Res* 1993;12:61–93.
6. Pasandideh-Fard M, Bhole R, Chandra S, Mostaghimi J. Capillary effects during droplet impact on a solid surface. *Phys Fluids* 1996;8:650–9.
7. Kim HY, Feng ZC, Chun JH. Instability of a liquid jet emerging from a droplet upon collision with a solid surface. *Phys Fluids* 2000;12:531–41.
8. Mehdizadeh NZ, Chandra S, Mostaghimi J. Formation of fingers around the edges of a drop hitting a metal plate with high velocity. *J Fluid Mech* 2004;510:353–73.
9. Hulse-Smith L, Mehdizadeh NZ, Chandra S. Deducing drop size and impact velocity from circular bloodstains. *J Forensic Sci* 2005;50(1):54–63.
10. Thoroddsen ST, Sakakibara J. Evolution of the fingering pattern of an impacting drop. *Phys Fluids* 1998;10:1359–74.

Additional information and reprint requests:

Lee Hulse-Smith, M.Sc.
 Centre of Forensic Sciences
 Biology Section, 4th Floor
 25 Grosvenor Street
 Toronto, ON
 Canada M7A 2G8
 E-mail: lee.hulsesmith@jus.gov.on.ca